PHASE EQUILIBRIA CONSTRAINTS ON MERCURY MELTING CONDITIONS. S.W. Parman[1], K.B. Williams[1,2], H.P. O'Brien[1], S. Wang[1], T.C. Prissel[1], E. M. Parmentier[1], P.C. Hess[1] and J.W. Head[1]. stephen_parman@brown.edu, [1]Department of Earth, Environmental and Planetary Sciences, Brown University, Providence, RI 02912, USA; [2]Department of Earth and Planetary Sciences, Washington University, St. Louis, MO 63130, USA

Introduction: Mercury's surface can broadly be divided into two main units [1]: 1) the northern smooth plains (NSP), which cover the northern polar region and from their morphology appear to be flood volcanics and 2) the inter-crater plains and highly cratered terrain (IcP-HCT), which cover most of the rest of the planet. The greater amount of cratering in the IcP-HCT indicate it is older (4.0-4.2 Ga) than the NSP (3.7-3.8 Ga), and also somewhat obscures the nature of the IcP-HCT, though much of it appears to be volcanic [2].

The compositions of these units has been constrained by x-ray fluorescence (XRS) on board the MESSENGER mission (Figure 1; [3,4]). While there is much overlap between the two terrains, in general, the NSP is has lower MgO and CaO, and higher SiO_2 and Al_2O_3.

We have performed high P and T experiments on an average NSP composition to determine the effect of low oxygen fugacities (log fO_2 ~ IW-3) on the phase equilbria of mafic melts, at sulfide saturated conditions. These results are compared to previous Mercury phase equilbria experiments [5-8].

Methods: The composition used is an average NSP composition (gray star in Figures 1 and 2, [4]). A synthetic version of it was made by mixing reagent grade oxides. Based on previous experiments, silicon was added as 95% SiO_2 and 5% Si metal, by weight, to produce a log fO_2 around IW-3 [8,9]. S was added as elemental S (1.2 wt%). The experiments were all run in an internally-heated gas pressure device at Brown University. Pressures were 186±14 bar and temperatures ranged from 1400-1225°C. Starting powders were contained in a graphite capsule, which was placed inside a Pt capsule and welded shut. Run durations were typically 24 to 48 hrs. At the end of the experiment, the charge was drop quenched. The sample was sectioned and polished using mineral spirits to avoid MgCa sulfide dissolution. All phases were analyzed using the Cameca SX100 microprobe at Brown University.

Experimental Results: The melt compositions are shown in Figure 1 (gray diamonds) and compared to previous mantle melting phase boundaries for terrestrial conditions (QFM, no S: gray dashed lines, [7]) and Mercury-like conditions (IW-3, sulfide saturated, black lines, [8]). The melt compositions define the olivine-protoenstatite (ol-prEn) boundary, which is shifted to higher quartz and anorthite compositions

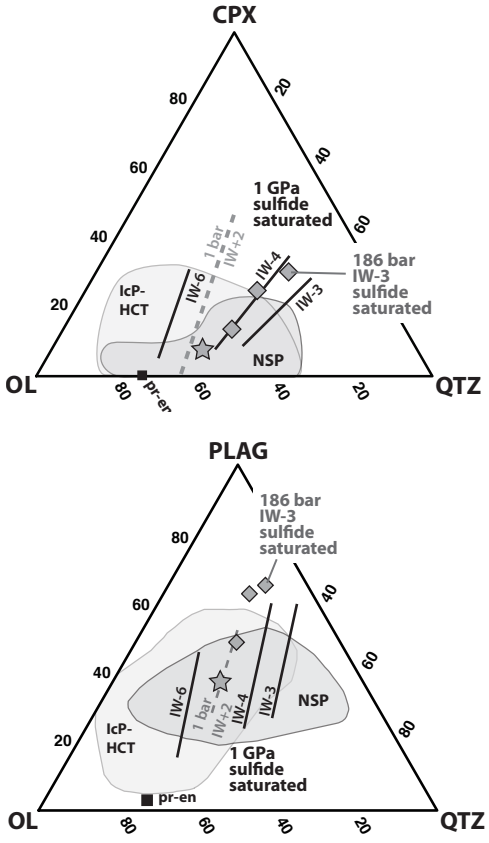

Figure 1: *Olivine-clinopyroxene-plagioclase-quartz ternary phase diagrams for melt compositions (gray diamonds) in crystallization experiments on an NSP composition (gray star) at 186 bar pressures, low fO_2 (IW-3) and sulfide saturated conditions. All of the melts are saturated with olivine, protoenstatite (black square) and a sulfide melt. This boundary is shifted to higher quartz and plagioclase contents relative to the ol-prEn boundary at higher oxygen fugacities (IW+2) and sulfide absent conditions (gray dashed line, 1 bar pressure, [7]). The ol-prEn phase boundaries for mantle melt experiments at 1 GPa (solid black lines) are also shifted to high qtz and plag compositions at oxygen fugacities above IW-5, but shift to lower values at fO_2 below that [8]. This corresponds to a shift in the composition of the sulfide melt from FeCr-rich to MgCa-rich (Figure 2). Compositions are shown in oxygen units. Composition of NSP and IcP-HCT from XRS [4] are shown as fields.*

relative to terrestrial data [7]. This is consistent with the results of Mercury mantle melting experiments at IW-3 to IW-4 [8].

Why the ol-prEn boundary shifts to higher SiO_2 and Al_2O_3 contents at fO_2 higher than IW-5 is not clear at this point. At lower fO_2 (below IW-5), the shift to lower SiO_2 can be understood as S bonding with Mg in the melt via the reaction:

$$Mg_2SiO_4+S = MgSiO_3+MgS+0.5O_2$$

This corresponds well with a shift in the composition of the equilibrium sulfide melt to higher Mg and Ca compositions (Figure 2).

The destabilization of anorthite could be due to Ca bonding with Ca via the reaction:

$$2CaAl_2Si_2O_8+2S+NaO_{0.5}= NaAlSi_3O_8+2CaS+SiO_2+3AlO_{1.5}+O_2$$

This might also explain the shift of the ol-prEn boundary to higher SiO_2 contents relative to the IW+2 boundary. This would suggest that even below IW-5, S is complexed with Ca in the melt. Interestingly, the 1 GPa phase ol-prEn boundary is shifted to even higher SiO_2 than the low pressure boundary, indicating expansion of the ol field at higher pressure, the reverse of what occurs at more terrestrial-like conditions [7].

Implications for melting/crystallization conditions: The high SiO_2 end of the NSP compositional spectrum is consistent with melting of a sulfide-saturated, enstatite-chondrite based Mercury mantle at oxygen fugacities 2 to 3 log units below IW and pressures of 1 GPa. The higher Mg end of the NSP compositional spectra are consistent with melting past the prEn-out boundary, leaving a dunite residue. At low pressure, NSP melts will crystallize olivine and prEn. These should be the dominant phenocryst phases in NSP lavas. None of the NSP compositions are feldspar saturated at low pressure (at IW-3 and sulfide saturated conditions). IcP-HCT compositions also show a wide range. At the high SiO_2 end, they are similar to NSP and could be explained by mantle melting of similar sources. However, the low SiO_2 end of the IcP-HCT compositional spectrum has higher CaO contents than the NSP melts and cannot be related by melting of the same source or by low pressure crystallization.

Implications for magma ocean crystallization: Crystallization of a Mercury magma ocean would initially be dominated by low-Ca pyroxene and to a lesser extent olivine. These will be essentially Fe-free and will have similar densities [10]. The complexing of S with Ca suppresses both plagioclase and clinopyroxene crystallization, which will allow the magma ocean to reach high Ca and Al compositions. This late stage magma ocean may be a good candidate to form the high Ca source required for the IcP-HCT lavas.

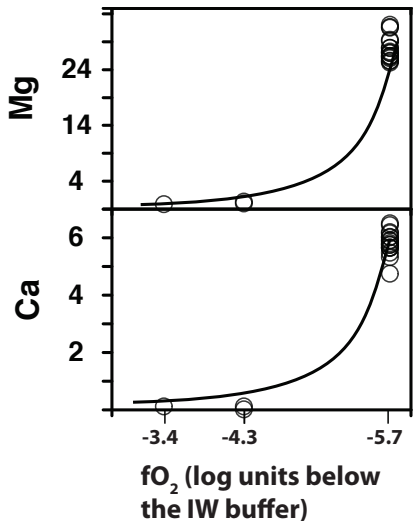

Figure 2. *Mg and Ca cation wt% in sulfide melts as a function of oxygen fugacity in 1 GPa mantle melting experiments [8]. The sulfides shift from FeCr rich to MgCa rich as fO_2 decreases below IW-5.*

Sulfide compositions and heat producing elements: Above log fO_2 of ~IW-5, sulfides will be FeCr-rich if these elements are present. However, such sulfides are very dense and should readily sink out of a crystallizing magma ocean, leaving it essentially Fe and Cr-free, forcing subsequent sulfides to be MgCa-rich. CaS has high partition coefficients for heat producing elements U, Th and K [11,12]. Thus the destabilization of Ca-bearing silicates should result in heat-producing elements being concentrated in Ca-sulfides in the latest crystallization products of the magma ocean. These should reside near the top of the mantle. Because the silicates are Fe-free, no density inversion or mantle overturn is expected, in contrast to the crystallization of the lunar magma ocean. Heat production from this shallow mantle layer could be an important cause of subsequent mantle melting.

Acknowledgements: We thank Joe Boesenberg for his assistance with the EMPA analyses.

References: **[1]** Head J.W. et al, (2011) Science, 333, 1853-1856, **[2]** Whitten J.L. et al, (2014), Icarus, 241, 97-113. **[3]** Nittler L.R. et al, (2011) Science, 333, 1847-1850 **[4]** Weider S.Z. et al, (2012), *JGR, 117*, E004153,**[5]** McCoy, T.J. et al, (1999) Meteoritics and Planet Sci, 34, 735-746. **[6]** Berthet S. et al, (2009), Geochim Cosmoschim Acta, 73, 6402-6420. **[7]** Charlier B. et al, (2013), EPSL 363, 50-60 **[8]** Parman, S.W. et al (2014), LPSC XXXV, 2367. **[9]** Zolotov M.Y. (2011) Icarus, 212, 24-41. **[10]** Brown S.M. & Elkins-Tanton L.T. (2009) EPSL 286, 446-455. **[11]** Floss C. et al (1990) Geochim Cosmoschim Acta 54, 3553-3558. **[12]** Murrell M.T. (1986) JGR 91, 8126-8136.